

Article

Application of OpenArray Technology to Assess Changes in the Expression of Functionally Significant Genes in the Substantia Nigra of Mice in a Model of Parkinson's Disease

Dmitry Troshev [†] , Anna Kolacheva [†] , Ekaterina Pavlova, Victor Blokhin  and Michael Ugrumov ^{*}

Laboratory of Neural and Neuroendocrine Regulations, Koltzov Institute of Developmental Biology of the Russian Academy of Sciences, 119334 Moscow, Russia; dmitry.vad.troshev@gmail.com (D.T.); annakolacheva@gmail.com (A.K.); guchia@gmail.com (E.P.); victor.blokhin@hotmail.com (V.B.)

^{*} Correspondence: michael.ugrumov@mail.ru

[†] These authors contributed equally to this work.

Abstract: Studying the molecular mechanisms of the pathogenesis of Parkinson's disease (PD) is critical to improve PD treatment. We used OpenArray technology to assess gene expression in the substantia nigra (SN) cells of mice in a 1-methyl-4-phenyl-1,2,3,6-tetrahydropyridine (MPTP) model of PD and in controls. Among the 11 housekeeping genes tested, *Rps27a* was taken as the reference gene due to its most stable expression in normal and experimental conditions. From 101 genes encoding functionally significant proteins of nigrostriatal dopaminergic neurons, 57 highly expressed genes were selected to assess their expressions in the PD model and in the controls. The expressions of *Th*, *Ddc*, *Maoa*, *Comt*, *Slc6a3*, *Slc18a2*, *Drd2*, and *Nr4a2* decreased in the experiment compared to the control, indicating decreases in the synthesis, degradation, and transport of dopamine and the impaired autoregulation of dopaminergic neurons. The expressions of *Tubb3*, *Map2*, *Syn1*, *Syt1*, *Rab7*, *Sod1*, *Cib1*, *Gpx1*, *Psmid4*, *Ubb*, *Usp47*, and *Ctsb* genes were also decreased in the MPTP-treated mice, indicating impairments of axonal and vesicular transport and abnormal functioning of the antioxidant and ubiquitin-proteasome systems in the SN. The detected decreases in the expressions of *Snca*, *Nsf*, *Dnm11*, and *Keap1* may serve to reduce pathological protein aggregation, increase dopamine release in the striatum, prevent mitophagy, and restore the redox status of SN cells.

Keywords: substantia nigra; mice; model of Parkinson's disease; MPTP; reference genes; OpenArray



Citation: Troshev, D.; Kolacheva, A.; Pavlova, E.; Blokhin, V.; Ugrumov, M. Application of OpenArray Technology to Assess Changes in the Expression of Functionally Significant Genes in the Substantia Nigra of Mice in a Model of Parkinson's Disease. *Genes* **2023**, *14*, 2202. <https://doi.org/10.3390/genes14122202>

Academic Editors: Emiliano Giardina and Stefania Zampatti

Received: 7 November 2023

Revised: 7 December 2023

Accepted: 11 December 2023

Published: 12 December 2023



Copyright: © 2023 by the authors. Licensee MDPI, Basel, Switzerland. This article is an open access article distributed under the terms and conditions of the Creative Commons Attribution (CC BY) license (<https://creativecommons.org/licenses/by/4.0/>).

1. Introduction

Parkinson's disease (PD) is a socially significant neurodegenerative disorder, ranking second in incidence and severity after Alzheimer's disease. It is characterized by the progressive degeneration of dopaminergic (DAergic) neurons in the substantia nigra (SN), a key regulator of motor function [1,2]. The number of patients with PD is growing rapidly [3] and is expected to increase from 4.1 million in 2005 to almost 8.7 million by 2030 [4]. PD diagnosis relies on the manifestation of specific motor symptoms (rigidity, bradykinesia, and tremor) [5–8], when up to 60% of DAergic neurons die in the SN, and the level of dopamine (DA) in the striatum decreases by 70–80% [1,9–11]. After the diagnosis of PD, patients are treated symptomatically with drugs containing L-DOPA and dopamine agonists. However, this treatment has limited effectiveness, since it does not slow down the progression of the disease and does not prevent the disability of patients [5,7,12–15].

From the above, it follows that one of the objectives facing neurologists, neuropharmacologists, and neurophysiologists is to improve the current treatment of PD. Based on the translational medicine paradigm, this is possible by elucidating the molecular mechanisms of neurodegeneration and neuroplasticity. Along with genetic mouse models of PD, treatment with neurotoxins is widely used for these investigations [16–19]. The most commonly

used models of this kind are based on the systemic administration of 1-methyl-4-phenyl-1,2,3,6-tetrahydropyridine (MPTP), the neurotoxin of DAergic neurons [17]. The molecular mechanisms of PD pathogenesis are studied in this model at three interconnected levels, evaluating the gene expressions of functionally significant proteins of nigrostriatal DAergic neurons [20–22] as well as the content and functional activities of these proteins [23–25].

The number of identified genes encoding proteins involved in the pathogenesis of PD is gradually increasing [25–28]. Moreover, in PD, the disruption of various metabolic systems in DAergic neurons of the SN, such as the protein degradation system and the antioxidant system, and the regulation of neurotrophic factors have been shown [29–32]. Therefore, when developing disease models and when testing potential drugs, it is necessary to evaluate the expressions of numerous genes related to different intracellular processes. In this context, the development of high-performance PCR methods for the simultaneous assessment of the expressions of many genes in individual small samples is of particular value [33–35].

OpenArray, developed by Thermo Fisher Scientific, is one of the high-performance RT-qPCR technologies [33]. A specific characteristic of this technology is that for each sample, gene amplification is carried out on a chip in a large number of microscopic arrays. Compared to RT-qPCR, microvolume amplification ensures high efficiency of the method with significant saving in reagents and time spent. Each chip can simultaneously assess the expressions of up to 112 genes in 24 samples. At the request of consumers, the manufacturer produces chips with a required set of primers, which, on the one hand, ensures the reproducibility of results obtained in different laboratories, and on the other hand, allows for the development of target chips for specific diagnostic or research purposes.

Even the detection of small changes in the gene expressions of functionally significant proteins is important for elucidating the molecular mechanisms of the pathogenesis of any disease [36]. To analyze the RT-qPCR results, it is necessary to know which genes can serve as reference genes (RGs). Indeed, the expressions of genes of interest should be assessed in relation to the reference ones. The expressions of reference genes should not reliably change in pathology, for example, during neurodegeneration in PD. They are called housekeeping genes (HKGs) [36,37], which are expressed in all cells of the body, and the proteins they encode are necessary for the normal functioning of the cell. However, the expressions of some HKGs may still change during neurodegeneration [38], which requires preliminary testing of the stability of HKG expression in each specific pathology. In addition, it should be taken into account that the most stable HKGs may differ in various brain regions in patients with PD and in mice models of PD [37]. In this regard, the choice of HKGs that will be used for comparison with the expressions of genes of interest is crucial for the correct interpretation of the RT-qPCR data [36].

Proceeding from the above, this study aimed to analyze the expressions of numerous genes encoding functionally significant proteins in SN cells in mice in normal conditions and in PD models using OpenArray. To carry this out, it was necessary to meet the following objectives: (1) select the most stably expressed HKGs based on the assay of their expressions in mice under normal conditions and in PD modeling and (2) evaluate changes in the expressions of numerous highly expressed genes in the SN of a mouse PD model.

2. Materials and Methods

2.1. Animals and Experimental Procedures

We used male C57BL/6 mice ($n = 16$) aged 8–12 weeks and weighing 22–25 g, obtained from the Stolbovaya nursery (SKMT RAMS, Stolbovaya, Moscow region, Russia). Animals were kept in standard laboratory vivarium conditions at a temperature of 21–23 °C and a light cycle of 12:12 h, and they had free access to food and water.

To model the clinical stage of PD (hereinafter referred to as PD modeling), mice were subcutaneously injected with MPTP (Sigma-Aldrich, St. Louis, MO, USA) 4 times at a single dose of 12 mg/kg with an interval of 2 h between injections ($n = 8$) [16]. The control group of animals was administered a 0.9% NaCl solution according to the same scheme ($n = 8$).

2.2. Collection of Biological Material

Biological material was collected two weeks after the administration of MPTP or 0.9% NaCl. Mice were anesthetized with isoflurane (Baxter, Deerfield, IL, USA) in a SomnoSuite anesthesia machine (Kent Scientific Corporation, Torrington, CT, USA), decapitated, and the brains were removed and cut along the midsagittal plane at a cold temperature. The striatum and SN were then excised from the brain under the control in a Leica M60 stereomicroscope (Leica Microsystems, Wetzlar, Germany). The locations of the striatum and SN were determined using the mouse brain atlas [39]. Striatum samples were weighed, and the striatum and SN were frozen in liquid nitrogen and stored at -70°C until processing for high-performance liquid chromatography with electrochemical detection (striatum) or RNA extraction (SN).

2.3. High-Performance Liquid Chromatography with Electrochemical Detection

High-performance liquid chromatography with electrochemical detection was used to determine the concentration of DA and DA metabolites in the striatum samples as previously described [24].

2.4. Reverse Transcription Quantitative Real-Time Polymerase Chain Reaction

Extraction of total RNA from the SN samples of mice in all groups and cDNA synthesis were carried out as described in our previous work [22].

RT-qPCR analysis was carried out using TaqMan Open Array RT PCR Custom Format 112 chips (Lot 37B6745, REF 4470756 Applied Biosystems, Waltham, MA, USA). This study assessed the expressions of 101 genes of interest and 11 HKGs (Table S1). For RT-qPCR, 250 ng/ μL cDNA was taken. Raw data analysis was performed using the QuantStudio 12K Flex software (version 1.3, Applied Biosystems, Waltham, MA, USA) and Excel (Microsoft Corporation, Redmond, WA, USA).

The stability of HKG expression in the SN under normal conditions and when modeling PD was assessed using the RefFinder program [40] based on the algorithms of the GeNorm [41], NormFinder [42], and BestKeeper programs [43] and the comparative ΔCt method [44]. This allowed us to rank stably expressed genes. Using the above algorithms, RefFinder was used to calculate the score for each gene and the geometric mean of their scores to determine the final gene ranking (<https://blooge.cn/RefFinder/?type=reference>, accessed on 23 October 2023). Stability of gene expression was assessed using a composite score for each gene in control and PD modeling. The closer the score is to 1, the more stable the gene expression is considered. For each HKGs, the total score was calculated as the sum of the comprehensive ranking values in the control and PD modeling.

Gene expression levels are expressed as $2^{-\Delta\Delta\text{Ct}}$ values normalized to the expression of *Rps27a* as an RG. Formulas (1) and (2) were used for calculating $\Delta\Delta\text{Ct}$ as follows:

$$\Delta\text{Ct} = (\text{Ct}(\text{gene}) - \text{Ct}(\text{Rps27a})) \quad (1)$$

$$\Delta\Delta\text{Ct} = (\Delta\text{Ct}(\text{sample}) - \Delta\text{Ct}(\text{medium control})) \quad (2)$$

The results were calculated as the geometric mean of the group [45].

2.5. Statistics

Statistical analysis was carried out using GraphPad Prism 9 software (version 9.5.1, GraphPad Software, Inc., La Jolla, CA, USA). The normality of the groups was assessed using the Shapiro–Wilk test. For pairwise comparison, the unpaired Student's *t*-test was used. The results are presented as mean \pm SEM. Differences were considered significant at $p \leq 0.05$.

3. Results and Discussion

3.1. Characteristics of the Parkinson's Disease Model

We used an acute mouse model of the clinical stage of PD that was previously developed in our laboratory [16]. This model reproduces the landmarks of the state of the nigrostriatal DAergic system in patients after the appearance of specific motor symptoms and diagnosis of the disease [1]. These include a decrease in the level of DA in the striatum by more than 70–80%, a loss of almost half of the DAergic neurons in the SN, and impaired motor behavior [16].

The correct reproduction of the PD model was tested in this work by the crucial indicator—a threshold decrease in the level of DA in the striatum. According to our data, the concentration of DA in the striatum of mice in the control group was 99 pmol/mg, and after the administration of MPTP, it decreased to 12 pmol/mg, which was 12% of the control level (Figure 1A). These data indicate the correct reproduction of the PD model.

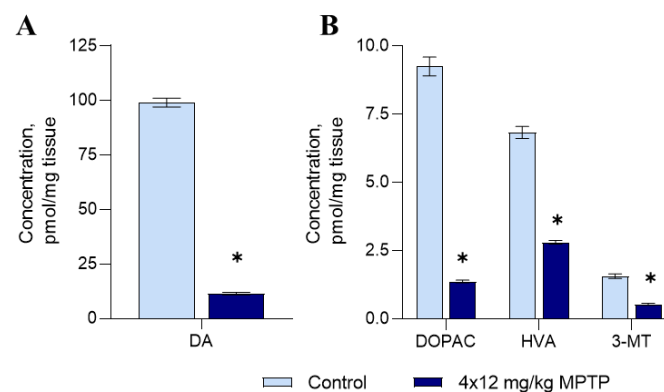


Figure 1. Concentrations of dopamine (DA) (A), 3,4-dihydroxyphenylacetic acid (DOPAC), homovanillic acid (HVA), and 3-methoxytyramine (3-MT) (B) in the striatum in a mouse model of Parkinson's disease. The Shapiro–Wilk test was used to assess the normal distribution of the groups. Statistics indicate significance via the unpaired *t*-test (* $p \leq 0.05$ compared with the control group). Data are presented as mean \pm SEM; $n = 8$ for each group.

Concentrations of DA metabolites, including 3,4-dihydroxyphenylacetic acid (DOPAC), 3-methoxytyramine (3-MT), and homovanillic acid (HVA), decreased in the striatum of MPTP-treated mice by 85%, 66%, and 59%, respectively (Figure 1B).

3.2. Selection of Stably Expressed Housekeeping Genes Based on Analysis of Their Expression in Normal Conditions and in Modeling Parkinson's Disease

Based on previous experience using RG in RT-qPCR [36,37,46–50], we selected 11 HKGs: X-prolyl aminopeptidase (aminopeptidase P) 1 (*Xpnpep1*), alanyl-tRNA synthetase (*Aars*), GTPase activating protein and VPS9 domains 1 (*Gapvd1*), oxysterol binding protein (*Osbp*), glyceraldehyde-3-phosphate dehydrogenase (*Gapdh*), succinate dehydrogenase complex, subunit A (*Sdha*), 40S ribosomal protein S27a (*Rps27a*), ubiquitin-conjugating enzyme E2D2 (*Ube2d2*), cytochrome C1 (*Cyc1*), ribosomal protein L13 (*Rpl13*), and hypoxanthine guanine phosphoribosyl transferase (*Hprt*). The stability of the expressions of some genes was previously shown in patients with PD and in animal models of PD [36,37,49]. However, the expressions of these genes have not always been assessed in SN [36,46], including SN in the mouse model of PD used in this work.

The stability of HKG expression in the SN of mice of the control and experimental groups was assessed using four methods proposed in RefFinder (comparative method $\Delta\Delta Ct$, BestKeeper, NormFinder, and GeNorm) (Table 1).

Table 1. Ranking of the stability of the expressions of housekeeping genes in the substantia nigra in mice under normal conditions and in model of Parkinson’s disease, calculated using the RefFinder software (<https://blogo.cn/RefFinder/?type=reference>, accessed on 23 October 2023).

Gene Rank	Control					4 × 12 mg/kg MPTP					Summary Score
	Comprehensive Ranking	Delta CT	BestKeeper	NormFinder	GeNorm	Comprehensive Ranking	Delta CT	BestKeeper	NormFinder	GeNorm	
	HKG/Score	HKG/Score	HKG/Score	HKG/Score	HKG/Score	HKG/Score	HKG/Score	HKG/Score	HKG/Score	HKG/Score	
1	<i>Rps27a</i> 1.41	<i>Sdha</i> 0.57	<i>Rps27a</i> 0.333	<i>Sdha</i> 0.253	<i>Rps27a</i> 0.389	<i>Rps27a</i> 1.68	<i>Cyc1</i> 2.95	<i>Rpl13</i> 0.333	<i>Ube2d2a</i> 0.226	<i>Rps27a</i> 0.452	<i>Rps27a</i> 3.09
2	<i>Sdha</i> 2.45	<i>Rps27a</i> 0.57	<i>Gapdh</i> 0.417	<i>Rps27a</i> 0.267	<i>Ube2d2a</i> 0.389	<i>Ube2d2a</i> 1.97	<i>Rps27a</i> 3.01	<i>Rps27a</i> 0.417	<i>Rps27a</i> 0.226	<i>Ube2d2a</i> 0.452	<i>Ube2d2a</i> 5.95
3	<i>Hprt</i> 3.72	<i>Gapvd1</i> 0.59	<i>Aars</i> 0.456	<i>Gapvd1</i> 0.328	<i>Hprt</i> 0.402	<i>Rpl13</i> 2.28	<i>Rpl13</i> 3.05	<i>Ube2d2a</i> 0.583	<i>Rpl13</i> 0.311	<i>Rpl13</i> 0.583	<i>Hprt</i> 8.15
4	<i>Gapvd1</i> 3.87	<i>Hprt</i> 0.62	<i>Hprt</i> 0.5	<i>Hprt</i> 0.390	<i>Sdha</i> 0.437	<i>Cyc1</i> 3.16	<i>Hprt</i> 3.07	<i>Hprt</i> 0.889	<i>Cyc1</i> 1.197	<i>Hprt</i> 0.836	<i>Cyc1</i> 8.85
5	<i>Ube2d2a</i> 3.98	<i>Cyc1</i> 0.64	<i>Gapvd1</i> 0.583	<i>Cyc1</i> 0.415	<i>Gapvd1</i> 0.471	<i>Hprt</i> 4.43	<i>Ube2d2a</i> 3.1	<i>Cyc1</i> 1.056	<i>Xpmp1</i> 1.655	<i>Cyc1</i> 0.979	<i>Sdha</i> 8.93
6	<i>Cyc1</i> 5.69	<i>Ube2d2a</i> 0.65	<i>Cyc1</i> 0.583	<i>Ube2d2a</i> 0.431	<i>Rpl13</i> 0.504	<i>Xpmp1</i> 6.19	<i>Xpmp1</i> 3.14	<i>Sdha</i> 1.306	<i>Hprt</i> 1.729	<i>Sdha</i> 1.084	<i>Rpl13</i> 9.24
7	<i>Aars</i> 6.26	<i>Rpl13</i> 0.67	<i>Ube2d2a</i> 0.583	<i>Rpl13</i> 0.476	<i>Cyc1</i> 0.530	<i>Sdha</i> 6.48	<i>Sdha</i> 3.21	<i>Xpmp1</i> 1.403	<i>Sdha</i> 2.189	<i>Xpmp1</i> 1.163	<i>Gapvd1</i> 13.87
8	<i>Gapdh</i> 6.69	<i>Aars</i> 0.71	<i>Rpl13</i> 0.611	<i>Aars</i> 0.538	<i>Aars</i> 0.560	<i>Gapdh</i> 8	<i>Gapdh</i> 3.33	<i>Gapdh</i> 1.667	<i>Gapdh</i> 2.216	<i>Gapdh</i> 1.259	<i>Gapdh</i> 14.69
9	<i>Rpl13</i> 6.96	<i>Xpmp1</i> 0.73	<i>Sdha</i> 0.625	<i>Xpmp1</i> 0.571	<i>Xpmp1</i> 0.580	<i>Aars</i> 9	<i>Aars</i> 3.42	<i>Aars</i> 1.75	<i>Aars</i> 2.593	<i>Aars</i> 1.303	<i>Aars</i> 15.26
10	<i>Xpmp1</i> 9.24	<i>Gapdh</i> 0.78	<i>Xpmp1</i> 0.625	<i>Gapdh</i> 0.623	<i>Gapdh</i> 0.616	<i>Gapvd1</i> 10	<i>Gapvd1</i> 8.95	<i>Gapvd1</i> 4.208	<i>Gapvd1</i> 8.064	<i>Gapvd1</i> 2.834	<i>Xpmp1</i> 15.43
11	<i>Oshp</i> 11	<i>Oshp</i> 0.98	<i>Oshp</i> 0.75	<i>Oshp</i> 0.889	<i>Oshp</i> 0.682	<i>Oshp</i> 11	<i>Oshp</i> 11.72	<i>Oshp</i> 7.806	<i>Oshp</i> 11.389	<i>Oshp</i> 4.449	<i>Oshp</i> 22

HKG—housekeeping gene; GRV—geometric mean of ranking values. Gene Rank—ranking from most stable to least stable gene. Comprehensive ranking—geometric mean calculated using a score of four methods: comparative Δ CT, NormFinder, BestKeeper, and GeNorm. Summary score—sum of values (score) of comprehensive ranking for HKGs in mice in control and in the model of Parkinson’s disease.

We have shown that among the selected HKGs, *Rps27a* has the most stable expression in both normal conditions and in the PD model. In addition to this gene, we identified five additional genes whose expressions were quite stable during neurodegeneration: *Ube2d2a*, *Hprt*, *Cyc1*, *Sdha*, and *Rpl13*. It is noteworthy that two of the six genes we selected, *Cyc1* and *Rpl13*, were previously used as RGs to assess gene expression with RT-qPCR in autopsy brain material from patients suffering from neurodegenerative diseases [36].

Based on the results obtained, we chose *Rps27a* as an RG to evaluate gene expression in the SN of a mouse model of PD. It should be noted that when choosing an RG, it is necessary to take into account what tissue, human pathology, and pathology models will be tested. For example, according to our data obtained on SN in the mouse model of PD, and according to the data obtained in a study of human skin cancer [50], *Rps27a* is considered a stably expressed gene that can be used as an RG in RT-qPCR. On the contrary, in multiple sclerosis, the expression of *Rps27a* changes, and it is considered a biomarker of the disease [51].

3.3. Assessing the Gene Expression Using OpenArray and Developing a Panel of Highly Expressed Genes

When developing the initial panel of genes of interest, we relied on previously obtained information on the molecular mechanisms of neurodegeneration and neuroplasticity, including changes in the gene expressions of functionally significant proteins, in the SN of patients with PD [28,52–59]. As a result, the initial panel consisted of 101 genes of proteins involved in the functioning of SN neurons and the pathogenesis of PD or, in other words, in the mechanisms of neurodegeneration and neuroplasticity.

The genes were collected into clusters according to the functions of the proteins they encode:

1. DA synthesis and degradation: Tyrosine hydroxylase (*Th*), dopa decarboxylase (*Ddc*), dopamine β -hydroxylase (*Dbh*), phenylethanolamine N-methyltransferase (*Pnmt*), monoamine oxidase A and B (*Maoa* and *Maob*), and catechol-O-methyltransferase (*Comt*);
2. DA transport, DA receptors, and transcriptional factors: DA transporter (*Slc6a3*), vesicular monoamine transporter 1 and 2 (*Slc18a1* and *Slc18a2*), plasma membrane monoamine

- transporter (*Slc29a4*), DA receptors 1–5 types (*Drd1–Drd5*), nuclear receptor subfamily 4 group A member 2 (*Nurr1*, *Nr4a2*); and paired-like homeodomain 3 (*Pitx3*);
3. Axonal transport and microtubules: Kinesin (*Kif1a*, *Kif1b*, *Kif5a*, and *Kif2c*), dynein (*Dync1h1* and *Dynll1*), dynactin 1 (*Dctn1*), tau-protein (*Mapt*), microtubule-associated protein 2 (*Map2*), MAP/microtubule affinity regulating kinase 2 (*Mark2*), and tubulin (*Tubb3*, *Tuba1a*);
 4. Vesicle cycle for neurotransmission: α -synuclein (*Snca*), synapsin 1 (*Syn1*), syntaxin 1A (*Stx1a*), synaptotagmin 1 and 11 (*Syt1*, *Syt11*), Rab protein 5a и 7 (*Rab5a*, *Rab7*), N-ethylmaleimide sensitive fusion protein (*Nsf*), dynamin 1-like protein (*Dnm1l*), and vacuolar protein sorting ortholog 35 (*Vps35*);
 5. Neuroprotection: Superoxide dismutase 1 (*Sod1*), glutathione peroxidase 1 (*Gpx1*), glutathione reductase (*Gsr*), thioredoxin reductase 1 (*Txnrd1*), nitric oxide synthase 1 (*Nos1*), peroxiredoxin 1 (*Prdx1*), nuclear factor erythroid 2-related factor 2 (*Nfe2l2*), angiotensin II receptor type 2 (*Agtr2*), sigma-1 receptor (*Sigmar1*), kelch-like ECH-associated protein 1 (*Keap1*), brain-derived neurotrophic factor (*Bdnf*), glial cell-derived neurotrophic factor (*Gdnf*), nerve growth factor (*Ngf*), vascular endothelial growth factor A (*Vegfa*), cerebral DA neurotrophic factor (*Cdnf*), neurotrophic tyrosine kinase receptor types 1 and 2 (*Ntrk1* and *Ntrk2*), nerve growth factor receptor (*Ngfr*), matrix metalloproteinase-3 (*Mmp3*), Wnt family member 11 (*Wnt11*), catenin β -1 (*Ctnnb1*), and calbindin 1 (*Calb1*);
 6. Protein degradation: Calcium channel voltage-dependent L type alpha 1D subunit (*Cacna1d*), transient receptor potential cation channel subfamily M member 2 (*Trpm2*), E3 ubiquitin ligase (Parkin) (*Park2*), ubiquitin-conjugating enzyme E2N (*Ube2n*), ubiquitin-like modifier activating enzyme 3 (*Uba3*), proteasome 20S subunit beta 4 (*Psmb4*), proteasome 26S subunit ATPase 3 (*Psmc3*), proteasome 26S subunit non-ATPase 4 (*Psmc4*), ubiquitin-specific peptidase 47 (*Usp47*), ubiquitin B (*Ubb*), and cathepsin B (*Ctsb*);
 7. Cell death: Caspases 1 and 3 (*Casp1* and *Casp3*), poly [ADP-ribose] polymerase 1 (*Parp1*), apoptosis-inducing factor mitochondria associated 1 (*Aifm1*), calcium and integrin binding 1 (*Cib1*), transformation-related protein 53 (*Trp53*), Bax protein (*Bax*), c-Fos protein (*Fos*), mitogen-activated protein kinase 8 (*Mapk8*), lysosomal-associated membrane protein 2 (*Lamp2*), autophagy-related 16-like 1 and 5 (*Atg16l1* and *Atg5*), calpain-1 (*Capn1*), tumor necrosis factor (*Tnf*), endoplasmic reticulum to nucleus signaling 2 (*Ern2*), eukaryotic translation initiation factor 2-alpha kinase 3 (*Ef2ak3*), and activating transcription factor 6 (*Atf6*);
 8. Inflammation and glial activation: Glial fibrillary acidic protein (*Gfap*), interferon gamma (*Ifng*), transforming growth factor beta 1 (*Tgfb1*), protein kinase B alpha (*Akt1*), cannabinoid receptor 1 (*Cnr1*), prostaglandin-endoperoxide synthase 2 (*Ptgs2*), CDC like kinase 1 (*Clk1*), transforming growth factor beta 1 (*Traf1*), C-X-C motif chemokine 11 (*Cxcl11*).

OpenArray, due to the use of a small sample volume in the microscopic arrays, is optimal for the evaluation of highly expressed genes when the amplification curve crosses the detection threshold before cycle 28 [60,61]. This is due to the fact that the probability of carrying out a PCR in each microscopic array in this case is at a maximum. It is methodologically incorrect to evaluate the expressions of lowly expressed genes (the amplification curve crosses the detection threshold between cycles 28 and 34) without additional preparatory procedures, as this leads to errors and a poor reproducibility of the results [33]. The preamplification of cDNA before OpenArray serves to reduce the cycle of crossing the detection threshold of the amplification curve (up to 10 cycles) without changing the results, which expands the range of analysis [34,62,63].

According to our data, in the SN, out of 101 genes included in the original panel, 57 have high levels of expression, 22 have low levels of expression, and we were unable to detect the expressions of 22 genes (Table 2). The latter may indicate the absence or very low expressions of these genes, in which the intersection of the amplification curve of

the detection threshold exceeds 34 cycles. The lack of expression in the SN of genes such as *Dbh*, *Pnmt*, and *Slc18a1* was expected, since they encode enzymes for the synthesis of norepinephrine, adrenaline, as well as vesicular monoamine transporter 1, which is characteristic of neuroendocrine cells [64]. In the SN, we also failed to detect the expressions of the genes for three DA receptors (*Drd3–Drd5*), the expression of *Kif2c*, which is involved in the depolymerization of microtubules in dendrites and regulates the invasion of microtubules into neuron spines when the neuronal activity changes [65], and the expressions of a number of genes from the “neuroprotection”, “cell death”, and “inflammation and glial activation” clusters (Table 2).

Table 2. Protein genes whose expressions were assessed in the substantia nigra of mice using TaqMan OpenArray RT-PCR custom chips.

Gene Clusters	Highly Expressed Genes (Can Be Detected with OpenArray)	Genes with Low Expressions (Can Be Detected with OpenArray Following Pre-amplification)	Genes with Very Low Expressions or Genes Not Expressed (Cannot Be Detected with OpenArray)
Synthesis and degradation of dopamine	<i>Th, Ddc, Comt, Maa, Maob</i>	-	<i>Dbh, Pnmt</i>
Dopamine transport, dopamine receptors, and transcription factors of dopaminergic neurons	<i>Slc18a2, Slc6a3, Drd2, Nr4a2</i>	<i>Slc29a4, Drd1</i>	<i>Drd3–Drd5, Slc18a1, Pitx3</i>
Axonal transport	<i>Tubb3, Tuba1a, Dynll1, Kif1a, Kif5a, Dctn1, Map2, Mapt</i>	<i>Kif1b, Dync1h1, Mark2</i>	<i>Kif2c</i>
Vesicular cycle and mediator release	<i>Syn1, Syt1, Snca, Syt11, Rab5a, Rab7, Dnm11, Vps35, Nsf</i>	<i>Stx1a</i>	-
Neuroprotection	<i>Gpx1, Gsr, Sod1, Prdx1, Txnrd1, Nfe2l2, Keap1, Sigmar1, Calb1, Ctnnb1, Ntrk2</i>	<i>Bdnf, Vegfa, Nos1, Agtr2</i>	<i>Ngf, Gdnf, Cdnf, Ntrk1, Mmp3, Wnt11, Ngfr</i>
Protein degradation	<i>Ubb, Uba3, Ube2n, Psmb4, Psm4, Psmc3, Usp47, Ctsb</i>	<i>Park2, Cacna1d, Trpm2</i>	-
Cell death	<i>Parp1, Cib1, Aifm1, Trp53, Lamp2, Mapk8, Atg5</i>	<i>Casp1, Casp3, Map3k5, Fos, Capn1, Eif2ak3, Atf6, Atg16l1</i>	<i>Tnf, Bcl2l11, Ern2</i>
Inflammation and glia activation	<i>Gfap, Clk1, Akt1, Cnr1</i>	<i>Tgfb1</i>	<i>Ifng, Cxcl11, Ptgs2, Traf1</i>

Gene names are indicated according to the National Library of Medicine GenBank (<https://www.ncbi.nlm.nih.gov/genbank> accessed on 4 November 2022).

Since OpenArray is best suited for assessing highly expressed genes, genes with low expressions were excluded from the final panel: *Slc29a4, Drd1, Kif1b, Mark2, Dync1h1, Stx1a, Vegfa, Bdnf, Nos1, Agtr2, Park2, Cacna1d, Trpm2, Casp1, Casp3, Map3k5, Fos, Capn1, Eif2ak3, Atf6, Atg16l1*, and *Tgfb1*. Thus, the final panel consisted of 57 genes with expressions that could be assessed in SN using OpenArray. However, we do not exclude that when modeling PD, the expression of some low-expressed genes encoding proteins involved in neuroprotection, cell death, inflammation, and glial activation may be higher than in animals in the control group.

3.4. Evaluation of Gene Expression in the Substantia Nigra in a Mouse Model of Parkinson’s Disease

The resulting panel, consisting of 57 genes, was used to study gene expression in SN in a mouse model of PD using OpenArray.

According to our data, in SN, the expressions of genes encoding DA-synthesizing enzymes (*Th* and *Ddc*) and DA transporters (*Slc6a3* and *Slc18a2*) are significantly reduced when modeling PD (Figure 2). At the same time, we showed that the expression of *Drd2*, encoding the D2 receptor, decreases in the SN in a model of PD. These data suggest a

decreased synthesis of the D2 receptor, an autoreceptor of DAergic neurons. Previously, using the same PD model, we studied the expressions of the *Th*, *Ddc*, *Slc6a3*, *Slc18a2*, and *Drd2* genes in the SN [23,66,67] and in the sorted DAergic neurons of the SN [22]. The complete coincidence in the expressions of these genes means that both approaches (RT-qPCR and OpenArray technology) give the same results. The remaining genes in the developed panel were first assessed in the SN in a model of an early clinical stage of PD.

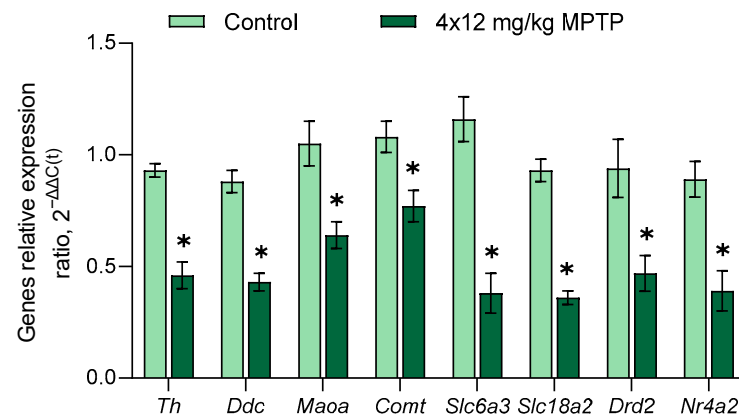


Figure 2. Changes in the expressions of genes encoding dopamine-synthesizing enzymes (*Th* and *Ddc*), dopamine-degrading enzymes (*Maa* and *Comt*), dopamine transporters (*Slc6a3* and *Slc18a2*), dopamine receptor (*Drd2*), and transcription factor Nurr1 (*Nr4a2*) in the substantia nigra in a mouse model of Parkinson’s disease. The Shapiro–Wilk test was used to assess the normal distribution of the groups. Statistics indicate significance by the unpaired *t*-test (* $p \leq 0.05$ compared with the control group). Data are presented as mean \pm SEM; $n = 8$ for each group.

Nr4a2 encodes the transcription factor Nurr1, which induces the expressions of genes of the DAergic phenotype in mesencephalic neurons [68,69]. *Th* expression is regulated directly by Nurr1, and the *Th* promoter has a binding site for Nurr1 [70,71]. This suggests a causal relationship between the decreased *Th* and *Nr4a2* expressions (Figure 2).

When modeling PD, we found a decrease in the expression of genes for enzymes that degrade DA: monoamine oxidase-A (*Maa*) and catechol-O-methyltransferase (*Comt*) (Figure 2). DA is degraded in two stages and along two metabolic pathways; each one involves both enzymes [72,73]. In the first stage, monoamine oxidase-A and aldehyde dehydrogenase convert DA into DOPAC, and catechol-O-methyltransferase converts DA into 3-MT. In the second stage, catechol-O-methyltransferase converts DOPAC into HVA, and monoamine oxidase-A and aldehyde dehydrogenase convert DOPAC into 3-MT. This means that decreased expressions of *Maa* and *Comt* may explain the decreased concentrations of DOPAC and 3-MT in the striatum. Considering that the concentration of DOPAC decreased to a greater extent than the concentration of 3-MT, we can conclude that DA degrades during PD modeling mainly in the extraneuronal space, where catechol-O-methyltransferase is localized [73]. In contrast to the monoamine oxidase-A gene, the expression of the monoamine oxidase-B gene (*Maob*) does not change in the PD model compared to the controls. This is probably explained by the fact that *Maa* is mainly expressed in neurons, whereas *Maob* is expressed in astrocytes [74].

When assessing the expressions of genes encoding axonal transport proteins, we showed a decrease in the expressions of *Map2* and *Tubb3* in the SN of mice in a model of PD (Figure 3). Microtubule-associated protein-2, encoded by the *Map2* gene, is localized primarily in neuronal dendrites. This protein stabilizes the assembly of microtubules and ensures their interaction with other components of the neuronal cytoskeleton [75–77]. In addition, in PD patients, this protein induces the formation of fibrous aggregates and crystal-like structures within the nuclei of neurons. It also colocalizes with α -synuclein and ubiquitin in cytoplasmic inclusion bodies [75]. β 3-tubulin is one of the structural proteins of microtubules, and mutations in the *Tubb3* can lead to the impaired production

of α/β heterodimers and thereby lead to a decrease in the stability of microtubules and the disruption of axonal transport [78]. β 3-tubulin found in the bloodstream is considered one of the nonspecific biomarkers of neurodegenerative diseases, including Alzheimer's disease and PD [79]. Decreases in the expressions of genes for proteins, including tubulins, kinesins, and dyneins, which are involved in anterograde and retrograde axonal transport, were previously shown in DAergic neurons of the SN of patients with PD [52]. Impaired axonal transport is considered an important characteristic of this disease [80,81]. Our results show that axonal transport is also impaired in PD models, as manifested by decreased expressions of genes encoding microtubule structural proteins and proteins regulating microtubule stability in the SN. This can lead to the disruption of the transport of organelles (mitochondria) and individual functionally important molecules along axons, promoting axonal degradation and neuronal death.

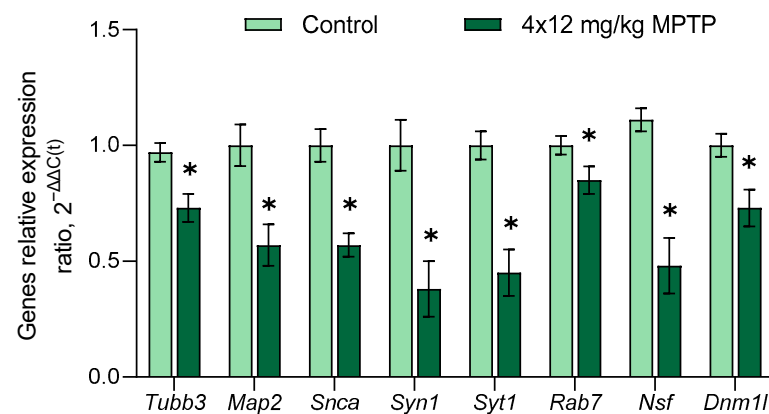


Figure 3. Changes in the expressions of genes for proteins associated with axonal transport (*Tubb3* and *Map2*) and the vesicular cycle (*Snca*, *Syn1*, *Syt1*, *Rab7*, *Nsf*, and *Dnm11*) in the substantia nigra in a mouse model of Parkinson's disease. The Shapiro–Wilk test was used to assess the normal distribution of the groups. Statistics indicate significance by the unpaired *t*-test (* $p \leq 0.05$ compared with the control group). Data are presented as mean \pm SEM. $n = 8$ for each group.

When assessing the expressions of genes encoding vesicular cycle proteins in the SN in a mouse model of PD, we observed decreases in the expressions of the following genes: *Snca*, *Syn1*, *Syt1*, *Rab7*, *Nsf*, and *Dnm11* (Figure 3). The *Snca* gene encodes α -synuclein, the presynaptic protein [82], and mutations of this gene lead to the development of PD [83,84]. The pathogenic neurotoxin is represented by prefibrillar α -synuclein, but not deposits of this protein—Lewy bodies. Oligomers or protofibrils of α -synuclein disrupt the normal degradation of proteins in the cell, which negatively affects the functioning of organelles such as the mitochondria and the endoplasmic reticulum [85,86]. It should be noted that α -synuclein oligomers can spread from neuron to neuron in a prion-like fashion via the intercellular space, thereby expanding the zone of neurodegeneration [82,85]. The decrease in *Snca* expression in the SN that we discovered, which was also shown in other studies when modeling PD in mice [87], may lead to a decrease in protein aggregation.

When studying the molecular mechanisms of the PD pathogenesis, the evaluation of DA neurotransmission, which is largely provided by vesicular cycle proteins, is of great importance. The *Syn1* gene encodes synapsin 1, a protein involved in the transport of synaptic vesicles and contributes to the regulation of synaptogenesis and axonogenesis [88]. The decrease in the expression of this gene in the SN in a mouse model of PD that we discovered may indicate a disruption in the transport of synaptic vesicles and, thus, synaptic neurotransmission. This was previously shown in a subchronic mouse model of the clinical stage of PD [89]. Another vesicular cycle protein is synaptotagmin 1, encoded by the *Syt1* gene. This protein is a calcium sensor involved in triggering the release of DA and other neurotransmitters from the synaptic terminals [90]. The decrease in *Syt1* expression that we found in the mouse PD model may suggest a decrease in DA neurotransmission in SN.

The third vesicular cycle protein, encoded by the *Rab7* gene, regulates the transport of late endosomes and autophagosomes, and its overexpression prevents the accumulation of the mutant A53T α -synuclein that was shown in the cell culture and in PD models in *Drosophila melanogaster* and rats [91,92]. The decrease in *Rab7* expression that we discovered during the modeling of PD indicates a decrease in the ability of SN cells to degrade pathological proteins in autophagosomes.

In response to the DAergic denervation of the striatum, compensatory processes are activated, aimed at minimizing DA deficiency in this part of the brain by increasing the functional activity of surviving DAergic neurons of the SN [93] and increasing the release of DA from their axonal terminals located in the striatum [94]. It should be noted that the presynaptic N-ethylmaleimide-sensitive hybrid protein encoded by the *Nsf* gene plays a fundamental role in synaptic neurotransmission. This protein is an ATPase, which couples ATP hydrolysis to the disassembly of SNARE proteins, allowing them to be included in the next round of synaptic vesicle exocytosis [95]. Increased ATPase activity of the N-ethylmaleimide-sensitive fusion protein is observed when it is phosphorylated by leucine-rich repeat kinase 2 at threonine 645 in the ATP-binding pocket of the D2 domain [95]. An N-ethylmaleimide-sensitive fusion protein is involved in the pathogenesis of some inherited forms of PD. Indeed, the *LRRK2* G2019S mutation in PD results in increased leucine-rich repeat kinase 2 activity, which increases the frequency of phosphorylation of the N-ethylmaleimide-sensitive fusion protein and leads to its accumulation in toxic inclusion bodies [96]. Since DA neurotransmission in the striatum is characterized by both the complete and partial fusion of synaptic vesicles with the plasma membrane according to the “kiss-and-run” mechanism, promoting the release of a small amount of DA into the synaptic cleft [97,98], it can be assumed that the decrease in *Nsf* expression that we discovered in this work contributes to a decrease in the synthesis of N-ethylmaleimide-sensitive fusion protein. This, in turn, can lead to the slower disassembly of SNARE proteins and hence an increase in the amount of DA released into the synaptic cleft. We believe that a decrease in *Nsf* gene expression may be one of the compensatory processes that develop in the SN when modeling PD.

The genes we studied also include *Dnm1l*, encoded dynamin-related protein 1, which is involved in mitochondrial fission and mitophagy [99]. The loss of the ability of mitochondria to divide due to the removal of dynamin-related protein leads to the degradation of DAergic axonal terminals in the striatum and contributes to the preferential death of nigral DAergic neurons [100]. A number of researchers emphasize the importance of Drp-1-dependent mitochondrial fragmentation to protect cells from death caused by aggregated α -synuclein [101]. At the same time, it was shown that the inhibition of the synthesis of dynamin-related protein 1 in MPTP-treated mice leads to a weakening of the toxic effect of MPTP and a restoration of the normal level of DA release in the striatum [102]. Based on these data, the decrease in *Dnm1l* expression in the SN that we observed in this study in a mouse model of PD seems to be a compensatory process that prevents mitophagy and protects existing mitochondria from degradation.

It is well known that the death of neurons is caused by oxidative stress due to the increased production of highly reactive oxygen, highly reactive nitrogen, cations of certain metals, and a decreased activity of the antioxidant system, i.e., an impairment of the “redox status” of the cell [103]. When modeling PD, we found decreases in the expressions of the *Sod1* and *Gpx1* genes, encoding enzymes of the antioxidant system—superoxide dismutase type 1 and glutathione peroxidase 1 (Figure 4). This fact is consistent with the data on an increase in the level of oxidative stress that were obtained when studying an autopsy of the SN in PD patients [104,105]. In PD, a decrease in the glutathione content by 40% in the SN, but not in other parts of the brain, has also been shown [106–108]. Taken together, the above data indicate a selective decrease in the activity of the antioxidant system in DAergic neurons of the SN in PD [108].

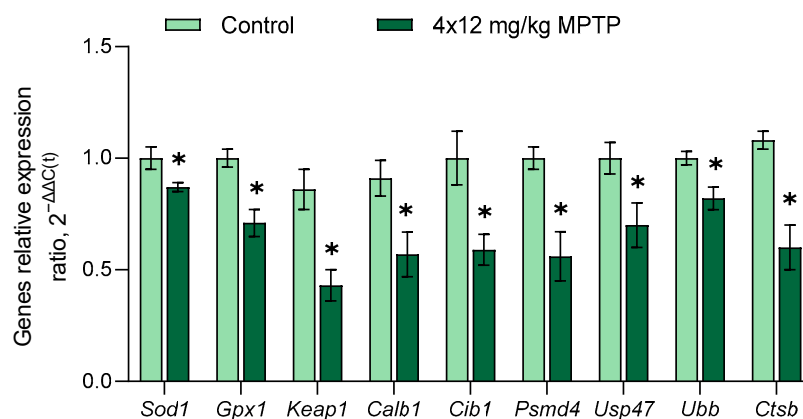


Figure 4. Changes in the expressions of genes encoding proteins of the antioxidant system (*Sod1* and *Gpx1*), transcription factors (*Keap1*), calcium-binding proteins (*Calb1* and *Cib1*) and proteins of the ubiquitin-proteasome system (*Psm4*, *Ubb*, *Usp47*, and *Ctsb*) in the substantia nigra in a mouse model of Parkinson’s disease. The Shapiro–Wilk test was used to assess the normal distribution of the groups. Statistics indicate significance using unpaired *t* test (* $p \leq 0.05$ vs. control group). Data are presented as mean \pm SEM; $n = 8$ for each group.

We showed a decrease in the expression of the *Keap1* gene, encoding ECH Kelch-associated protein 1, associated with the transcription factor Nrf2b, in the SN of mice models of PD (Figure 4) [109,110]. Under oxidative stress or low *Keap1* expression, Nrf2 dissociates from ECH Kelch binding protein 1 and translocates to the nucleus, where it activates the expression of antioxidant system genes [111]. We assume that the decrease in *Keap1* expression is a compensatory process aimed at restoring the “redox status” of degenerating neurons.

When studying the mechanisms that contribute to the partial compensation of DA deficiency in the striatum when modeling PD, it is of particular interest to study the expressions of genes encoding calcium-binding proteins. Indeed, we found a decrease in the expression of *Calb1*, which encodes calbindin 1 protein. This protein binds calcium in the cytoplasm, protecting the cell from the cytotoxic effect of calcium [112]. It is logical to assume that the decrease in *Calb1* gene expression that we discovered, probably accompanied by a decrease in the synthesis of calbindin 1, may be a compensatory process aimed at stimulating DA release from striatal DAergic axons when modeling PD. However, it was previously shown that calbindin 1 regulates DA release and uptake in the ventral rather than the dorsal striatum, which is involved in the regulation of motor behavior [113]. Therefore, in the future, it will be desirable to elucidate the role of calbindin 1 in DA neurotransmission and compensatory processes in the dorsal striatum during the development of PD.

In addition, we showed a decrease in the expression of *Cib1* (Figure 4), encoding another calcium-binding protein, calcium- and integrin-binding protein 1, which has been shown to be involved in a wide range of intracellular processes, such as the regulation of microtubule formation during cell division [114] and the regulation of β -amyloid production by controlling the subcellular localization of γ -secretase [115]. It was previously shown that calcium- and integrin-binding protein 1 inhibits the activity of signal-regulating kinase 1, which prevents the apoptosis of DAergic neurons in the SN in PD modeling using 6-hydroxydopamine and MPTP [116,117]. In this regard, the decrease in the expression of the *Cib1* gene, which we found in the SN when modeling PD, may indicate a decrease in the ability of cells in this area of the brain to prevent apoptotic cell death.

It is well known that neurotrophic factors play important roles in the regulation of brain development and reparative processes in brain damage. This prompted the present study to evaluate the gene expressions of neurotrophic factors, neurotrophic factor receptors, and transcription factors involved in the activation of signaling pathways that may promote the survival of DAergic neurons in a mouse model of PD. However, according to our data, the expression of the *Ntrk2* gene, encoding the receptor for BDNF, does

not change in the MPTP-treated mice. These data are in good agreement with previous pathological studies showing that the expression of *Ntrk2* does not change in patients with PD [53]. This is also the case for genes of neurotrophic factors, their receptors, and transcription factors involved in activation signaling pathways that promote the survival of DAergic neurons [52]. Thus, in PD patients and in animal models of clinical PD, there are no changes in the expressions of neurotrophic factors, neurotrophic factor receptors, and transcription factors involved in the activation of signaling pathways that may promote the survival of DAergic neurons. This indicates that with the significant death of SN DAergic neurons, which is characteristic of the clinical stage of PD, neurotrophic factors are not involved in the regulation of reparative processes associated with the degradation of the nigrostriatal DAergic system.

When evaluating the expressions of genes for proteins undergoing proteasomal and lysosomal degradation, we found decreased expressions of *Psm4*, *Ubb*, *Usp47*, and *Ctsb* in the MPTP-treated mice (Figure 4). Since the ubiquitin–proteasome system ensures the degradation of misfolded and damaged proteins, its disruption leads to the accumulation of toxic proteins, including aggregated α -synuclein in PD [118]. The decreases in the expressions of genes encoding proteins of the 26S subunit of the proteasome (not ATPase 4) (*Psm4*), ubiquitin-specific peptidase 47 (*Usp47*), ubiquitin B (*Ubb*), and cathepsin B (*Ctsb*) that we discovered in mice models of PD may be accompanied by decreased synthesis and impaired degradation of these proteins in SN cells. Our data are in good agreement with those showing decreases in the expressions of genes for proteins of the ubiquitin–proteasome system in nigral DAergic neurons in PD patients [52].

The mechanism of neuronal death depends on the regime of MPTP administration to mice, and the observed changes in gene expression depend on how long after exposure to the neurotoxin the analysis is carried out [67,119]. In acute models of PD, when MPTP is administered for one day, necroptosis predominates, while with subchronic or chronic regimes of neurotoxin administration, other types of cell death, mainly apoptosis, predominate [17,120–122]. In this case, DAergic neurons degenerate no more than two days after the administration of the neurotoxin [123,124]. Therefore, with the experimental design used (sample collection 2 weeks after MPTP administration), we did not expect to observe any changes in the expressions of genes associated with neuronal death.

4. Conclusions

Thus, in this study, among 11 HKGs, we selected *Rps27a* as the most stably expressed gene in the control and MPTP-treated mice. Of the 101 protein genes involved in the functioning of SN neurons in normal conditions and in PD modeling, 57 genes with high expressions were selected for their subsequent analyses using OpenArray technology. We showed decreases in the expressions of genes encoding proteins involved in the synthesis, degradation, transport of DA, and autoregulation of DAergic neurons. When modeling PD, the expressions of genes for proteins of axonal and vesicular transport, as well as proteins of the antioxidant and ubiquitin–proteasome systems, were also reduced in the SN. Simultaneous decreases in the expressions of *Snca*, *Nsf*, *Dnm11*, and *Keap1* were shown in the MPTP-treated mice, which suggests the activation of compensatory processes in PD. These processes can serve to reduce the aggregation of pathological proteins, increase the release of dopamine in the striatum, inhibit mitophagy, and restore the “redox status” of SN cells. Undoubtedly, the knowledge about the molecular mechanisms of neurodegeneration and neuroplasticity of the nigrostriatal system that we obtained in a model of the early clinical stage of PD will be used for further research on this topic.

Supplementary Materials: The following supporting information can be downloaded at <https://www.mdpi.com/article/10.3390/genes14122202/s1>, Table S1: Genes and their target names on RT-qPCR chips for OpenArray technology.

Author Contributions: Conceptualization, D.T., A.K. and M.U.; methodology, D.T., A.K. and E.P.; formal analysis, D.T., A.K. and E.P.; investigation, A.K., E.P. and V.B.; writing—original draft prepa-

ration, D.T. and A.K.; writing—review and editing, M.U. and E.P.; visualization, A.K.; supervision, M.U.; project administration, M.U.; funding acquisition, M.U. All authors have read and agreed to the published version of the manuscript.

Funding: This research was funded by the Ministry of Science and Higher Education of the Russian Federation (grant agreement No 075-15-2020-795, state contract No 13.1902.21.0027 of 29.09.2020, unique project ID: RF-190220×0027).

Institutional Review Board Statement: All experiments were conducted in accordance with the NIH Guide for the Care and Use of Laboratory Animals and were approved by the Animal Care and Use Committee of the Koltzov Institute of Developmental Biology RAS (protocol no. 62 from 01.09.2022).

Informed Consent Statement: Not applicable.

Data Availability Statement: The data presented in this study are available upon request from the corresponding author. The data are not publicly available due to legal issues.

Acknowledgments: We are grateful for open access to the RefFinder resource (<https://blooge.cn/RefFinder/?type=reference> (accessed on 23 October 2023)).

Conflicts of Interest: The authors declare no conflict of interest. The funders had no role in the design, execution, interpretation, or writing of the study.

Abbreviations

3-MT	3-methoxytyramine
DA	dopamine
DAergic	dopaminergic
DOPAC	3,4-dihydroxyphenylacetic acid
HKG	housekeeping gene
HVA	homovanillic acid
MPTP	1-methyl-4-phenyl-1,2,3,6-tetrahydropyridine
PD	Parkinson's disease
RG	reference gene
RT-qPCR	Reverse-transcription quantitative real-time polymerase chain reaction
SN	substantia nigra

References

1. Agid, Y. Parkinson's Disease: Pathophysiology. *Lancet* **1991**, *337*, 1321–1324. [[CrossRef](#)]
2. Eriksen, J.L.; Wszolek, Z.; Petrucelli, L. Molecular Pathogenesis of Parkinson Disease. *Arch. Neurol.* **2005**, *62*, 353–357. [[CrossRef](#)] [[PubMed](#)]
3. GBD 2016 Disease and Injury Incidence and Prevalence Collaborators Global, Regional, and National Incidence, Prevalence, and Years Lived with Disability for 328 Diseases and Injuries for 195 Countries, 1990–2016: A Systematic Analysis for the Global Burden of Disease Study 2016. *Lancet* **2017**, *390*, 1211–1259. [[CrossRef](#)]
4. Dorsey, E.R.; Constantinescu, R.; Thompson, J.P.; Biglan, K.M.; Holloway, R.G.; Kieburtz, K.; Marshall, F.J.; Ravina, B.M.; Schifitto, G.; Siderowf, A.; et al. Projected Number of People with Parkinson Disease in the Most Populous Nations, 2005 through 2030. *Neurology* **2007**, *68*, 384–386. [[CrossRef](#)] [[PubMed](#)]
5. Olanow, C.W.; Tatton, W.G. Etiology and Pathogenesis of Parkinson's Disease. *Annu. Rev. Neurosci.* **1999**, *22*, 123–144. [[CrossRef](#)] [[PubMed](#)]
6. Gandhi, S.; Wood, N.W. Molecular Pathogenesis of Parkinson's Disease. *Hum. Mol. Genet.* **2005**, *14*, 2749–2755. [[CrossRef](#)]
7. Müller, T. Safinamide for Symptoms of Parkinson's Disease. *Drugs Today* **2015**, *51*, 653–659. [[CrossRef](#)]
8. Cacabelos, R. Parkinson's Disease: From Pathogenesis to Pharmacogenomics. *Int. J. Mol. Sci.* **2017**, *18*, 551. [[CrossRef](#)]
9. Kalia, L.V.; Lang, A.E. Parkinson's Disease. *Lancet* **2015**, *386*, 896–912. [[CrossRef](#)]
10. Postuma, R.B.; Berg, D. Advances in Markers of Prodromal Parkinson Disease. *Nat. Rev. Neurol.* **2016**, *12*, 622–634. [[CrossRef](#)]
11. Blesa, J.; Trigo-Damas, I.; Dileone, M.; Del Rey, N.L.-G.; Hernandez, L.F.; Obeso, J.A. Compensatory Mechanisms in Parkinson's Disease: Circuits Adaptations and Role in Disease Modification. *Exp. Neurol.* **2017**, *298*, 148–161. [[CrossRef](#)] [[PubMed](#)]
12. Fabbrini, G.; Brotchie, J.M.; Grandas, F.; Nomoto, M.; Goetz, C.G. Levodopa-Induced Dyskinesias. *Mov. Disord.* **2007**, *22*, 1379–1389. [[CrossRef](#)]
13. Chotibut, T.; Fields, V.; Salvatore, M.F. Norepinephrine Transporter Inhibition with Desipramine Exacerbates L-DOPA-Induced Dyskinesia: Role for Synaptic Dopamine Regulation in Denervated Nigrostriatal Terminals. *Mol. Pharmacol.* **2014**, *86*, 675–685. [[CrossRef](#)]

14. Malek, N. Deep Brain Stimulation in Parkinson's Disease. *Neurol. India* **2019**, *67*, 968–978. [[CrossRef](#)] [[PubMed](#)]
15. Kwon, D.K.; Kwatra, M.; Wang, J.; Ko, H.S. Levodopa-Induced Dyskinesia in Parkinson's Disease: Pathogenesis and Emerging Treatment Strategies. *Cells* **2022**, *11*, 3736. [[CrossRef](#)] [[PubMed](#)]
16. Ugrumov, M.V.; Khaindrava, V.G.; Kozina, E.A.; Kucheryanu, V.G.; Bocharov, E.V.; Kryzhanovsky, G.N.; Kudrin, V.S.; Narkevich, V.B.; Klodt, P.M.; Rayevsky, K.S.; et al. Modeling of Presymptomatic and Symptomatic Stages of Parkinsonism in Mice. *Neuroscience* **2011**, *181*, 175–188. [[CrossRef](#)] [[PubMed](#)]
17. Jackson-Lewis, V.; Przedborski, S. Protocol for the MPTP Mouse Model of Parkinson's Disease. *Nat. Protoc.* **2007**, *2*, 141–151. [[CrossRef](#)] [[PubMed](#)]
18. Lama, J.; Buhidma, Y.; Fletcher, E.J.R.; Duty, S. Animal Models of Parkinson's Disease: A Guide to Selecting the Optimal Model for Your Research. *Neuronal Signal.* **2021**, *5*, NS20210026. [[CrossRef](#)]
19. Jagmag, S.A.; Tripathi, N.; Shukla, S.D.; Maiti, S.; Khurana, S. Evaluation of Models of Parkinson's Disease. *Front. Neurosci.* **2015**, *9*, 503. [[CrossRef](#)]
20. Bye, C.R.; Jönsson, M.E.; Björklund, A.; Parish, C.L.; Thompson, L.H. Transcriptome Analysis Reveals Transmembrane Targets on Transplantable Midbrain Dopamine Progenitors. *Proc. Natl. Acad. Sci. USA* **2015**, *112*, E1946–E1955. [[CrossRef](#)]
21. Agarwal, D.; Sandor, C.; Volpato, V.; Caffrey, T.M.; Monzón-Sandoval, J.; Bowden, R.; Alegre-Abarrategui, J.; Wade-Martins, R.; Webber, C. A Single-Cell Atlas of the Human Substantia Nigra Reveals Cell-Specific Pathways Associated with Neurological Disorders. *Nat. Commun.* **2020**, *11*, 4183. [[CrossRef](#)]
22. Troshev, D.; Blokhin, V.; Ukrainskaya, V.; Kolacheva, A.; Ugrumov, M. Isolation of Living Dopaminergic Neurons Labeled with a Fluorescent Ligand of the Dopamine Transporter from Mouse Substantia Nigra as a New Tool for Basic and Applied Research. *Front. Mol. Neurosci.* **2022**, *15*, 1020070. [[CrossRef](#)] [[PubMed](#)]
23. Mingazov, E.R.; Khakimova, G.R.; Kozina, E.A.; Medvedev, A.E.; Buneeva, O.A.; Bazyan, A.S.; Ugrumov, M.V. MPTP Mouse Model of Preclinical and Clinical Parkinson's Disease as an Instrument for Translational Medicine. *Mol. Neurobiol.* **2018**, *55*, 2991–3006. [[CrossRef](#)] [[PubMed](#)]
24. Kolacheva, A.; Alekperova, L.; Pavlova, E.; Bannikova, A.; Ugrumov, M.V. Changes in Tyrosine Hydroxylase Activity and Dopamine Synthesis in the Nigrostriatal System of Mice in an Acute Model of Parkinson's Disease as a Manifestation of Neurodegeneration and Neuroplasticity. *Brain Sci.* **2022**, *12*, 779. [[CrossRef](#)]
25. Coku, I.; Mutez, E.; Eddarkaoui, S.; Carrier, S.; Marchand, A.; Deldycke, C.; Goveas, L.; Baille, G.; Tir, M.; Magnez, R.; et al. Functional Analyses of Two Novel LRRK2 Pathogenic Variants in Familial Parkinson's Disease. *Mov. Disord.* **2022**, *37*, 1761–1767. [[CrossRef](#)] [[PubMed](#)]
26. Ichinose, H.; Ohye, T.; Fujita, K.; Pantucek, F.; Lange, K.; Riederer, P.; Nagatsu, T. Quantification of mRNA of Tyrosine Hydroxylase and Aromatic L-Amino Acid Decarboxylase in the Substantia Nigra in Parkinson's Disease and Schizophrenia. *J. Neural Transm. Park. Dis. Dement. Sect.* **1994**, *8*, 149–158. [[CrossRef](#)] [[PubMed](#)]
27. Noureddine, M.A.; Li, Y.-J.; van der Walt, J.M.; Walters, R.; Jewett, R.M.; Xu, H.; Wang, T.; Walter, J.W.; Scott, B.L.; Hulette, C.; et al. Genomic Convergence to Identify Candidate Genes for Parkinson Disease: SAGE Analysis of the Substantia Nigra. *Mov. Disord.* **2005**, *20*, 1299–1309. [[CrossRef](#)]
28. Duke, D.C.; Moran, L.B.; Pearce, R.K.B.; Graeber, M.B. The Medial and Lateral Substantia Nigra in Parkinson's Disease: mRNA Profiles Associated with Higher Brain Tissue Vulnerability. *Neurogenetics* **2007**, *8*, 83–94. [[CrossRef](#)]
29. Chang, K.-H.; Chen, C.-M. The Role of Oxidative Stress in Parkinson's Disease. *Antioxidants* **2020**, *9*, 597. [[CrossRef](#)]
30. Calabresi, P.; Mechelli, A.; Natale, G.; Volpicelli-Daley, L.; Di Lazzaro, G.; Ghiglieri, V. α -Synuclein in Parkinson's Disease and Other Synucleinopathies: From Overt Neurodegeneration Back to Early Synaptic Dysfunction. *Cell Death Dis.* **2023**, *14*, 176. [[CrossRef](#)]
31. Bondarenko, O.; Saarma, M. Neurotrophic Factors in Parkinson's Disease: Clinical Trials, Open Challenges and Nanoparticle-Mediated Delivery to the Brain. *Front. Cell. Neurosci.* **2021**, *15*, 682597. [[CrossRef](#)] [[PubMed](#)]
32. McNaught, K.S.; Jenner, P. Proteasomal Function Is Impaired in Substantia Nigra in Parkinson's Disease. *Neurosci. Lett.* **2001**, *297*, 191–194. [[CrossRef](#)]
33. Abraham, N.A.; Campbell, A.C.; Hirst, W.D.; Nezich, C.L. Optimization of Small-Scale Sample Preparation for High-Throughput OpenArray Analysis. *J. Biol. Methods* **2021**, *8*, e143. [[CrossRef](#)] [[PubMed](#)]
34. Li, P.; Grigorenko, E.; Funari, V.; Enright, E.; Zhang, H.; Kim, H.L. Evaluation of a High-Throughput, Microfluidics Platform for Performing TaqMan™ qPCR Using Formalin-Fixed Paraffin-Embedded Tumors. *Bioanalysis* **2013**, *5*, 1623–1633. [[CrossRef](#)] [[PubMed](#)]
35. Lamas, A.; Franco, C.M.; Regal, P.; Miranda, J.M.; Vázquez, B.; Cepeda, A.; Lamas, A.; Franco, C.M.; Regal, P.; Miranda, J.M.; et al. High-Throughput Platforms in Real-Time PCR and Applications. In *Polymerase Chain Reaction for Biomedical Applications*; IntechOpen: London, UK, 2016; ISBN 978-953-51-2796-3.
36. Rydbirk, R.; Folke, J.; Winge, K.; Aznar, S.; Pakkenberg, B.; Brudek, T. Assessment of Brain Reference Genes for RT-qPCR Studies in Neurodegenerative Diseases. *Sci. Rep.* **2016**, *6*, 37116. [[CrossRef](#)]
37. Alieva, A.K.; Filatova, E.V.; Rudenok, M.M.; Slominsky, P.A.; Shadrina, M.I. Housekeeping Genes for Parkinson's Disease in Humans and Mice. *Cells* **2021**, *10*, 2252. [[CrossRef](#)] [[PubMed](#)]

38. Maruyama, W.; Akao, Y.; Youdim, M.B.; Davis, B.A.; Naoi, M. Transfection-Enforced Bcl-2 Overexpression and an Anti-Parkinson Drug, Rasagiline, Prevent Nuclear Accumulation of Glyceraldehyde-3-Phosphate Dehydrogenase Induced by an Endogenous Dopaminergic Neurotoxin, N-Methyl(R)Salsolinol. *J. Neurochem.* **2001**, *78*, 727–735. [[CrossRef](#)]
39. Paxinos and Franklin's the Mouse Brain in Stereotaxic Coordinates—5th Edition. Available online: <https://shop.elsevier.com/books/paxinos-and-franklins-the-mouse-brain-in-stereotaxic-coordinates/paxinos/978-0-12-816157-9> (accessed on 12 October 2023).
40. Xie, F.; Wang, J.; Zhang, B. RefFinder: A Web-Based Tool for Comprehensively Analyzing and Identifying Reference Genes. *Funct. Integr. Genomics* **2023**, *23*, 125. [[CrossRef](#)]
41. Vandesompele, J.; De Preter, K.; Pattyn, F.; Poppe, B.; Van Roy, N.; De Paepe, A.; Speleman, F. Accurate Normalization of Real-Time Quantitative RT-PCR Data by Geometric Averaging of Multiple Internal Control Genes. *Genome Biol.* **2002**, *3*, RESEARCH0034. [[CrossRef](#)]
42. Andersen, C.L.; Jensen, J.L.; Ørntoft, T.F. Normalization of Real-Time Quantitative Reverse Transcription-PCR Data: A Model-Based Variance Estimation Approach to Identify Genes Suited for Normalization, Applied to Bladder and Colon Cancer Data Sets. *Cancer Res.* **2004**, *64*, 5245–5250. [[CrossRef](#)]
43. Pfaffl, M.W.; Tichopad, A.; Prgomet, C.; Neuvians, T.P. Determination of Stable Housekeeping Genes, Differentially Regulated Target Genes and Sample Integrity: BestKeeper—Excel-Based Tool Using Pair-Wise Correlations. *Biotechnol. Lett.* **2004**, *26*, 509–515. [[CrossRef](#)] [[PubMed](#)]
44. Silver, N.; Best, S.; Jiang, J.; Thein, S.L. Selection of Housekeeping Genes for Gene Expression Studies in Human Reticulocytes Using Real-Time PCR. *BMC Mol. Biol.* **2006**, *7*, 33. [[CrossRef](#)] [[PubMed](#)]
45. Anglade, P.; Vyas, S.; Javoy-Agid, F.; Herrero, M.T.; Michel, P.P.; Marquez, J.; Mouatt-Prigent, A.; Ruberg, M.; Hirsch, E.C.; Agid, Y. Apoptosis and Autophagy in Nigral Neurons of Patients with Parkinson's Disease. *Histol. Histopathol.* **1997**, *12*, 25–31. [[PubMed](#)]
46. Coulson, D.T.R.; Brockbank, S.; Quinn, J.G.; Murphy, S.; Ravid, R.; Irvine, G.B.; Johnston, J.A. Identification of Valid Reference Genes for the Normalization of RT qPCR Gene Expression Data in Human Brain Tissue. *BMC Mol. Biol.* **2008**, *9*, 46. [[CrossRef](#)] [[PubMed](#)]
47. Penna, I.; Vella, S.; Gigoni, A.; Russo, C.; Cancedda, R.; Pagano, A. Selection of Candidate Housekeeping Genes for Normalization in Human Postmortem Brain Samples. *Int. J. Mol. Sci.* **2011**, *12*, 5461–5470. [[CrossRef](#)]
48. De Spiegelaere, W.; Dern-Wieloch, J.; Weigel, R.; Schumacher, V.; Schorle, H.; Nettersheim, D.; Bergmann, M.; Brehm, R.; Kliesch, S.; Vandekerckhove, L.; et al. Reference Gene Validation for RT-qPCR, a Note on Different Available Software Packages. *PLoS ONE* **2015**, *10*, e0122515. [[CrossRef](#)] [[PubMed](#)]
49. Verma, A.; Kommaddi, R.P.; Gnanabharathi, B.; Hirsch, E.C.; Ravindranath, V. Genes Critical for Development and Differentiation of Dopaminergic Neurons Are Downregulated in Parkinson's Disease. *J. Neural Transm.* **2023**, *130*, 495–512. [[CrossRef](#)]
50. Hoang, V.L.T.; Tom, L.N.; Quek, X.-C.; Tan, J.-M.; Payne, E.J.; Lin, L.L.; Sinnya, S.; Raphael, A.P.; Lambie, D.; Frazer, I.H.; et al. RNA-Seq Reveals More Consistent Reference Genes for Gene Expression Studies in Human Non-Melanoma Skin Cancers. *PeerJ* **2017**, *5*, e3631. [[CrossRef](#)]
51. Chen, X.; Hou, H.; Qiao, H.; Fan, H.; Zhao, T.; Dong, M. Identification of Blood-Derived Candidate Gene Markers and a New 7-Genes Diagnostic Model for Multiple Sclerosis. *Biol. Res.* **2021**, *54*, 12. [[CrossRef](#)]
52. Simunovic, F.; Yi, M.; Wang, Y.; Macey, L.; Brown, L.T.; Krichevsky, A.M.; Andersen, S.L.; Stephens, R.M.; Benes, F.M.; Sonntag, K.C. Gene Expression Profiling of Substantia Nigra Dopamine Neurons: Further Insights into Parkinson's Disease Pathology. *Brain* **2009**, *132*, 1795–1809. [[CrossRef](#)]
53. Zaccaria, A.; Antinori, P.; Licker, V.; Kövari, E.; Lobrinus, J.A.; Burkhard, P.R. Multiomic Analyses of Dopaminergic Neurons Isolated from Human Substantia Nigra in Parkinson's Disease: A Descriptive and Exploratory Study. *Cell Mol. Neurobiol.* **2022**, *42*, 2805–2818. [[CrossRef](#)]
54. Hauser, M.A.; Li, Y.-J.; Xu, H.; Nouredine, M.A.; Shao, Y.S.; Gullans, S.R.; Scherzer, C.R.; Jensen, R.V.; McLaurin, A.C.; Gibson, J.R.; et al. Expression Profiling of Substantia Nigra in Parkinson Disease, Progressive Supranuclear Palsy, and Frontotemporal Dementia with Parkinsonism. *Arch. Neurol.* **2005**, *62*, 917–921. [[CrossRef](#)]
55. Moran, L.B.; Duke, D.C.; Deprez, M.; Dexter, D.T.; Pearce, R.K.B.; Graeber, M.B. Whole Genome Expression Profiling of the Medial and Lateral Substantia Nigra in Parkinson's Disease. *Neurogenetics* **2006**, *7*, 1–11. [[CrossRef](#)] [[PubMed](#)]
56. Cantuti-Castelvetri, I.; Keller-McGandy, C.; Bouzou, B.; Asteris, G.; Clark, T.W.; Frosch, M.P.; Standaert, D.G. Effects of Gender on Nigral Gene Expression and Parkinson Disease. *Neurobiol. Dis.* **2007**, *26*, 606–614. [[CrossRef](#)] [[PubMed](#)]
57. Simunovic, F.; Yi, M.; Wang, Y.; Stephens, R.; Sonntag, K.C. Evidence for Gender-Specific Transcriptional Profiles of Nigral Dopamine Neurons in Parkinson Disease. *PLoS ONE* **2010**, *5*, e8856. [[CrossRef](#)]
58. Elstner, M.; Morris, C.M.; Heim, K.; Bender, A.; Mehta, D.; Jaros, E.; Klopstock, T.; Meitinger, T.; Turnbull, D.M.; Prokisch, H. Expression Analysis of Dopaminergic Neurons in Parkinson's Disease and Aging Links Transcriptional Dysregulation of Energy Metabolism to Cell Death. *Acta Neuropathol.* **2011**, *122*, 75–86. [[CrossRef](#)]
59. Glaab, E.; Schneider, R. Comparative Pathway and Network Analysis of Brain Transcriptome Changes during Adult Aging and in Parkinson's Disease. *Neurobiol. Dis.* **2015**, *74*, 1–13. [[CrossRef](#)] [[PubMed](#)]
60. Prokopec, S.D.; Watson, J.D.; Waggott, D.M.; Smith, A.B.; Wu, A.H.; Okey, A.B.; Pohjanvirta, R.; Boutros, P.C. Systematic Evaluation of Medium-Throughput mRNA Abundance Platforms. *RNA* **2013**, *19*, 51–62. [[CrossRef](#)]
61. Morrison, T.; Hurley, J.; Garcia, J.; Yoder, K.; Katz, A.; Roberts, D.; Cho, J.; Kanigan, T.; Ilyin, S.E.; Horowitz, D.; et al. Nanoliter High Throughput Quantitative PCR. *Nucleic Acids Res.* **2006**, *34*, e123. [[CrossRef](#)]

62. Patel, S.N.; Wu, Y.; Bao, Y.; Mancebo, R.; Au-Young, J.; Grigorenko, E. TaqMan[®] OpenArray[®] High-Throughput Transcriptional Analysis of Human Embryonic and Induced Pluripotent Stem Cells. *Methods Mol. Biol.* **2013**, *997*, 191–201. [[CrossRef](#)]
63. Dalgard, C.L.; Polston, K.F.; Sukumar, G.; Mallon, C.T.M.; Wilkerson, M.D.; Pollard, H.B. MicroRNA Expression Profiling of the Armed Forces Health Surveillance Branch Cohort for Identification of “Enviro-miRs” Associated With Deployment-Based Environmental Exposure. *J. Occup. Environ. Med.* **2016**, *58*, S97–S103. [[CrossRef](#)] [[PubMed](#)]
64. Erickson, J.D.; Schafer, M.K.; Bonner, T.I.; Eiden, L.E.; Weihe, E. Distinct Pharmacological Properties and Distribution in Neurons and Endocrine Cells of Two Isoforms of the Human Vesicular Monoamine Transporter. *Proc. Natl. Acad. Sci. USA* **1996**, *93*, 5166–5171. [[CrossRef](#)] [[PubMed](#)]
65. Zheng, R.; Du, Y.; Wang, X.; Liao, T.; Zhang, Z.; Wang, N.; Li, X.; Shen, Y.; Shi, L.; Luo, J.; et al. KIF2C Regulates Synaptic Plasticity and Cognition in Mice through Dynamic Microtubule Depolymerization. *eLife* **2022**, *11*, e72483. [[CrossRef](#)] [[PubMed](#)]
66. Kozina, E.A.; Khakimova, G.R.; Khaindrava, V.G.; Kucheryanu, V.G.; Vorobyeva, N.E.; Krasnov, A.N.; Georgieva, S.G.; Kerkerian-Le Goff, L.; Ugrumov, M.V. Tyrosine Hydroxylase Expression and Activity in Nigrostriatal Dopaminergic Neurons of MPTP-Treated Mice at the Presymptomatic and Symptomatic Stages of Parkinsonism. *J. Neurol. Sci.* **2014**, *340*, 198–207. [[CrossRef](#)]
67. Alieva, A.K.; Filatova, E.V.; Kolacheva, A.A.; Rudenok, M.M.; Slominsky, P.A.; Ugrumov, M.V.; Shadrina, M.I. Transcriptome Profile Changes in Mice with MPTP-Induced Early Stages of Parkinson’s Disease. *Mol. Neurobiol.* **2017**, *54*, 6775–6784. [[CrossRef](#)] [[PubMed](#)]
68. Castillo, S.O.; Baffi, J.S.; Palkovits, M.; Goldstein, D.S.; Kopin, I.J.; Witta, J.; Magnuson, M.A.; Nikodem, V.M. Dopamine Biosynthesis Is Selectively Abolished in Substantia Nigra/Ventral Tegmental Area but Not in Hypothalamic Neurons in Mice with Targeted Disruption of the Nurr1 Gene. *Mol. Cell. Neurosci.* **1998**, *11*, 36–46. [[CrossRef](#)] [[PubMed](#)]
69. Chu, Y.; Kompoliti, K.; Cochran, E.J.; Mufson, E.J.; Kordower, J.H. Age-Related Decreases in Nurr1 Immunoreactivity in the Human Substantia Nigra. *J. Comp. Neurol.* **2002**, *450*, 203–214. [[CrossRef](#)]
70. Iwawaki, T.; Kohno, K.; Kobayashi, K. Identification of a Potential Nurr1 Response Element That Activates the Tyrosine Hydroxylase Gene Promoter in Cultured Cells. *Biochem. Biophys. Res. Commun.* **2000**, *274*, 590–595. [[CrossRef](#)]
71. Kim, K.-S.; Kim, C.-H.; Hwang, D.-Y.; Seo, H.; Chung, S.; Hong, S.J.; Lim, J.-K.; Anderson, T.; Isacson, O. Orphan Nuclear Receptor Nurr1 Directly Transactivates the Promoter Activity of the Tyrosine Hydroxylase Gene in a Cell-Specific Manner. *J. Neurochem.* **2003**, *85*, 622–634. [[CrossRef](#)]
72. López-Pérez, S.J.; Morales-Villagrán, A.; Medina-Ceja, L. Effect of Perinatal Asphyxia and Carbamazepine Treatment on Cortical Dopamine and DOPAC Levels. *J. Biomed. Sci.* **2015**, *22*, 14. [[CrossRef](#)]
73. Juárez Olguín, H.; Calderón Guzmán, D.; Hernández García, E.; Barragán Mejía, G. The Role of Dopamine and Its Dysfunction as a Consequence of Oxidative Stress. *Oxid. Med. Cell Longev.* **2016**, *2016*, 9730467. [[CrossRef](#)]
74. Levitt, P.; Maxwell, G.D.; Pintar, J.E. Specific Cellular Expression of Monoamine Oxidase B during Early Stages of Quail Embryogenesis. *Dev. Biol.* **1985**, *110*, 346–361. [[CrossRef](#)]
75. D’Andrea, M.R.; Ilyin, S.; Plata-Salaman, C.R. Abnormal Patterns of Microtubule-Associated Protein-2 (MAP-2) Immunolabeling in Neuronal Nuclei and Lewy Bodies in Parkinson’s Disease Substantia Nigra Brain Tissues. *Neurosci. Lett.* **2001**, *306*, 137–140. [[CrossRef](#)] [[PubMed](#)]
76. Dehmelt, L.; Halpain, S. The MAP2/Tau Family of Microtubule-Associated Proteins. *Genome Biol.* **2005**, *6*, 204. [[CrossRef](#)]
77. Nishida, K.; Matsumura, K.; Tamura, M.; Nakamichi, T.; Shimamori, K.; Kuragano, M.; Kabir, A.M.R.; Kakugo, A.; Kotani, S.; Nishishita, N.; et al. Effects of Three Microtubule-Associated Proteins (MAP2, MAP4, and Tau) on Microtubules’ Physical Properties and Neurite Morphology. *Sci. Rep.* **2023**, *13*, 8870. [[CrossRef](#)] [[PubMed](#)]
78. Poirier, K.; Saillour, Y.; Bahi-Buisson, N.; Jaglin, X.H.; Fallet-Bianco, C.; Nabbout, R.; Castelnaud-Ptakhine, L.; Roubertie, A.; Attie-Bitach, T.; Desguerre, I.; et al. Mutations in the Neuronal SS-Tubulin Subunit TUBB3 Result in Malformation of Cortical Development and Neuronal Migration Defects. *Hum. Mol. Genet.* **2010**, *19*, 4462–4473. [[CrossRef](#)] [[PubMed](#)]
79. Salama, M.; Shalash, A.; Magdy, A.; Makar, M.; Roushdy, T.; Elbalkimy, M.; Elrassas, H.; Elkafrawy, P.; Mohamed, W.; Abou Donia, M.B. Tubulin and Tau: Possible Targets for Diagnosis of Parkinson’s and Alzheimer’s Diseases. *PLoS ONE* **2018**, *13*, e0196436. [[CrossRef](#)] [[PubMed](#)]
80. Guo, W.; Stoklund Dittlau, K.; Van Den Bosch, L. Axonal Transport Defects and Neurodegeneration: Molecular Mechanisms and Therapeutic Implications. *Semin. Cell Dev. Biol.* **2020**, *99*, 133–150. [[CrossRef](#)]
81. Yang, X.; Ma, Z.; Lian, P.; Xu, Y.; Cao, X. Common Mechanisms Underlying Axonal Transport Deficits in Neurodegenerative Diseases: A Mini Review. *Front. Mol. Neurosci.* **2023**, *16*, 1172197. [[CrossRef](#)]
82. Stefanis, L. α -Synuclein in Parkinson’s Disease. *Cold Spring Harb. Perspect. Med.* **2012**, *2*, a009399. [[CrossRef](#)]
83. Polymeropoulos, M.H.; Higgins, J.J.; Golbe, L.I.; Johnson, W.G.; Ide, S.E.; Di Iorio, G.; Sanges, G.; Stenroos, E.S.; Pho, L.T.; Schaffer, A.A.; et al. Mapping of a Gene for Parkinson’s Disease to Chromosome 4q21-Q23. *Science* **1996**, *274*, 1197–1199. [[CrossRef](#)]
84. Polymeropoulos, M.H.; Lavedan, C.; Leroy, E.; Ide, S.E.; Dehejia, A.; Dutra, A.; Pike, B.; Root, H.; Rubenstein, J.; Boyer, R.; et al. Mutation in the α -Synuclein Gene Identified in Families with Parkinson’s Disease. *Science* **1997**, *276*, 2045–2047. [[CrossRef](#)] [[PubMed](#)]
85. Ingelsson, M. α -Synuclein Oligomers—Neurotoxic Molecules in Parkinson’s Disease and Other Lewy Body Disorders. *Front. Neurosci.* **2016**, *10*, 408. [[CrossRef](#)] [[PubMed](#)]
86. Cascella, R.; Chen, S.W.; Bigi, A.; Camino, J.D.; Xu, C.K.; Dobson, C.M.; Chiti, F.; Cremades, N.; Cecchi, C. The Release of Toxic Oligomers from α -Synuclein Fibrils Induces Dysfunction in Neuronal Cells. *Nat. Commun.* **2021**, *12*, 1814. [[CrossRef](#)] [[PubMed](#)]

87. Rudenok, M.M.; Shadrina, M.I.; Filatova, E.V.; Rybolovlev, I.N.; Nesterov, M.S.; Abaimov, D.A.; Ageldinov, R.A.; Kolacheva, A.A.; Ugrumov, M.V.; Slominsky, P.A.; et al. Expression Analysis of Genes Involved in Transport Processes in Mice with MPTP-Induced Model of Parkinson's Disease. *Life* **2022**, *12*, 751. [[CrossRef](#)] [[PubMed](#)]
88. Mirza, F.J.; Zahid, S. The Role of Synapsins in Neurological Disorders. *Neurosci. Bull.* **2017**, *34*, 349–358. [[CrossRef](#)] [[PubMed](#)]
89. Kolacheva, A.; Pavlova, E.; Bannikova, A.; Bogdanov, V.; Troshev, D.; Ugrumov, M. The Gene Expression of Proteins Involved in Intercellular Signaling and Neurodegeneration in the Substantia Nigra in a Mouse Subchronic Model of Parkinson's Disease. *Int. J. Mol. Sci.* **2023**, *24*, 3027. [[CrossRef](#)] [[PubMed](#)]
90. Kershberg, L.; Banerjee, A.; Kaeser, P.S. Protein Composition of Axonal Dopamine Release Sites in the Striatum. *eLife* **2022**, *11*, e83018. [[CrossRef](#)]
91. Dinter, E.; Saridaki, T.; Nippold, M.; Plum, S.; Diederichs, L.; Komnig, D.; Fensky, L.; May, C.; Marcus, K.; Voigt, A.; et al. Rab7 Induces Clearance of α -Synuclein Aggregates. *J. Neurochem.* **2016**, *138*, 758–774. [[CrossRef](#)]
92. Szegö, E.M.; Van den Haute, C.; Höfs, L.; Baekelandt, V.; Van der Perren, A.; Falkenburger, B.H. Rab7 Reduces α -Synuclein Toxicity in Rats and Primary Neurons. *Exp. Neurol.* **2022**, *347*, 113900. [[CrossRef](#)]
93. Hollerman, J.R.; Grace, A.A. The Effects of Dopamine-Depleting Brain Lesions on the Electrophysiological Activity of Rat Substantia Nigra Dopamine Neurons. *Brain Res.* **1990**, *533*, 203–212. [[CrossRef](#)] [[PubMed](#)]
94. Kirchoff, J.; Mørk, A.; Brennum, L.T.; Sager, T.N. Striatal Extracellular Dopamine Levels and Behavioural Reversal in MPTP-Lesioned Mice. *Neuroreport* **2009**, *20*, 482–486. [[CrossRef](#)] [[PubMed](#)]
95. Belluzzi, E.; Gonnelli, A.; Cîrnaru, M.-D.; Marté, A.; Plotegher, N.; Russo, I.; Civiero, L.; Cogo, S.; Carrion, M.P.; Franchin, C.; et al. LRRK2 Phosphorylates Pre-Synaptic N-Ethylmaleimide Sensitive Fusion (NSF) Protein Enhancing Its ATPase Activity and SNARE Complex Disassembling Rate. *Mol. Neurodegener.* **2016**, *11*, 1. [[CrossRef](#)] [[PubMed](#)]
96. Pischedda, F.; Cîrnaru, M.D.; Ponzoni, L.; Sandre, M.; Biossa, A.; Carrion, M.P.; Marin, O.; Morari, M.; Pan, L.; Greggio, E.; et al. LRRK2 G2019S Kinase Activity Triggers Neurotoxic NSF Aggregation. *Brain* **2021**, *144*, 1509–1525. [[CrossRef](#)]
97. Staal, R.G.W.; Mosharov, E.V.; Sulzer, D. Dopamine Neurons Release Transmitter via a Flickering Fusion Pore. *Nat. Neurosci.* **2004**, *7*, 341–346. [[CrossRef](#)]
98. Sulzer, D.; Cragg, S.J.; Rice, M.E. Striatal Dopamine Neurotransmission: Regulation of Release and Uptake. *Basal Ganglia* **2016**, *6*, 123–148. [[CrossRef](#)]
99. Feng, S.-T.; Wang, Z.-Z.; Yuan, Y.-H.; Wang, X.-L.; Sun, H.-M.; Chen, N.-H.; Zhang, Y. Dynamin-Related Protein 1: A Protein Critical for Mitochondrial Fission, Mitophagy, and Neuronal Death in Parkinson's Disease. *Pharmacol. Res.* **2020**, *151*, 104553. [[CrossRef](#)]
100. Berthet, A.; Margolis, E.B.; Zhang, J.; Hsieh, I.; Zhang, J.; Hnasko, T.S.; Ahmad, J.; Edwards, R.H.; Sesaki, H.; Huang, E.J.; et al. Loss of Mitochondrial Fission Depletes Axonal Mitochondria in Midbrain Dopamine Neurons. *J. Neurosci.* **2014**, *34*, 14304–14317. [[CrossRef](#)]
101. Martínez, J.H.; Fuentes, F.; Vanasco, V.; Alvarez, S.; Alaimo, A.; Cassina, A.; Coluccio Leskow, F.; Velazquez, F. α -Synuclein Mitochondrial Interaction Leads to Irreversible Translocation and Complex I Impairment. *Arch. Biochem. Biophys.* **2018**, *651*, 1–12. [[CrossRef](#)]
102. Rappold, P.M.; Cui, M.; Grima, J.C.; Fan, R.Z.; de Mesy-Bentley, K.L.; Chen, L.; Zhuang, X.; Bowers, W.J.; Tieu, K. Drp1 Inhibition Attenuates Neurotoxicity and Dopamine Release Deficits in Vivo. *Nat. Commun.* **2014**, *5*, 5244. [[CrossRef](#)]
103. Dias, V.; Junn, E.; Mouradian, M.M. The Role of Oxidative Stress in Parkinson's Disease. *J. Parkinsons Dis.* **2013**, *3*, 461–491. [[CrossRef](#)] [[PubMed](#)]
104. Wypijewska, A.; Galazka-Friedman, J.; Bauminger, E.R.; Wszolek, Z.K.; Schweitzer, K.J.; Dickson, D.W.; Jaklewicz, A.; Elbaum, D.; Friedman, A. Iron and Reactive Oxygen Species Activity in Parkinsonian Substantia Nigra. *Park. Relat. Disord.* **2010**, *16*, 329–333. [[CrossRef](#)] [[PubMed](#)]
105. Toulorge, D.; Schapira, A.H.V.; Hajj, R. Molecular Changes in the Postmortem Parkinsonian Brain. *J. Neurochem.* **2016**, *139* (Suppl. S1), 27–58. [[CrossRef](#)] [[PubMed](#)]
106. Perry, T.L.; Yong, V.W. Idiopathic Parkinson's Disease, Progressive Supranuclear Palsy and Glutathione Metabolism in the Substantia Nigra of Patients. *Neurosci. Lett.* **1986**, *67*, 269–274. [[CrossRef](#)] [[PubMed](#)]
107. Jenner, P.; Dexter, D.T.; Sian, J.; Schapira, A.H.; Marsden, C.D. Oxidative Stress as a Cause of Nigral Cell Death in Parkinson's Disease and Incidental Lewy Body Disease. The Royal Kings and Queens Parkinson's Disease Research Group. *Ann. Neurol.* **1992**, *32*, S82–S87. [[CrossRef](#)] [[PubMed](#)]
108. Sian, J.; Dexter, D.T.; Lees, A.J.; Daniel, S.; Agid, Y.; Javoy-Agid, F.; Jenner, P.; Marsden, C.D. Alterations in Glutathione Levels in Parkinson's Disease and Other Neurodegenerative Disorders Affecting Basal Ganglia. *Ann. Neurol.* **1994**, *36*, 348–355. [[CrossRef](#)] [[PubMed](#)]
109. Kansanen, E.; Kuosmanen, S.M.; Leinonen, H.; Levonen, A.-L. The Keap1-Nrf2 Pathway: Mechanisms of Activation and Dysregulation in Cancer. *Redox Biol.* **2013**, *1*, 45–49. [[CrossRef](#)] [[PubMed](#)]
110. Baird, L.; Yamamoto, M. The Molecular Mechanisms Regulating the KEAP1-NRF2 Pathway. *Mol. Cell. Biol.* **2020**, *40*, e00099-20. [[CrossRef](#)]
111. Taguchi, K.; Motohashi, H.; Yamamoto, M. Molecular Mechanisms of the Keap1-Nrf2 Pathway in Stress Response and Cancer Evolution. *Genes Cells* **2011**, *16*, 123–140. [[CrossRef](#)]

112. Rintoul, G.L.; Raymond, L.A.; Baimbridge, K.G. Calcium Buffering and Protection from Excitotoxic Cell Death by Exogenous Calbindin-D28k in HEK 293 Cells. *Cell Calcium* **2001**, *29*, 277–287. [[CrossRef](#)]
113. Brimblecombe, K.R.; Vietti-Michelina, S.; Platt, N.J.; Kastli, R.; Hnieno, A.; Gracie, C.J.; Cragg, S.J. Calbindin-D28K Limits Dopamine Release in Ventral but Not Dorsal Striatum by Regulating Ca²⁺ Availability and Dopamine Transporter Function. *ACS Chem. Neurosci.* **2019**, *10*, 3419–3426. [[CrossRef](#)] [[PubMed](#)]
114. Naik, M.U.; Naik, U.P. Calcium- and Integrin-Binding Protein 1 Regulates Microtubule Organization and Centrosome Segregation through Polo like Kinase 3 during Cell Cycle Progression. *Int. J. Biochem. Cell Biol.* **2011**, *43*, 120–129. [[CrossRef](#)] [[PubMed](#)]
115. Chiu, Y.W.; Hori, Y.; Ebinuma, I.; Sato, H.; Hara, N.; Ikeuchi, T.; Tomita, T. Identification of Calcium and Integrin-Binding Protein 1 as a Novel Regulator of Production of Amyloid β Peptide Using CRISPR/Cas9-Based Screening System. *FASEB J.* **2020**, *34*, 7661–7674. [[CrossRef](#)]
116. Yoon, K.W.; Cho, J.-H.; Lee, J.K.; Kang, Y.-H.; Chae, J.S.; Kim, Y.M.; Kim, J.; Kim, E.K.; Kim, S.E.; Baik, J.-H.; et al. CIB1 Functions as a Ca²⁺-Sensitive Modulator of Stress-Induced Signaling by Targeting ASK1. *Proc. Natl. Acad. Sci. USA* **2009**, *106*, 17389–17394. [[CrossRef](#)] [[PubMed](#)]
117. Yoon, K.W.; Yang, H.-S.; Kim, Y.M.; Kim, Y.; Kang, S.; Sun, W.; Naik, U.P.; Parise, L.V.; Choi, E.-J. CIB1 Protects against MPTP-Induced Neurotoxicity through Inhibiting ASK1. *Sci. Rep.* **2017**, *7*, 12178. [[CrossRef](#)] [[PubMed](#)]
118. Olanow, C.W.; Obeso, J.A.; Stocchi, F. Continuous Dopamine-Receptor Treatment of Parkinson’s Disease: Scientific Rationale and Clinical Implications. *Lancet Neurol.* **2006**, *5*, 677–687. [[CrossRef](#)] [[PubMed](#)]
119. Mandel, S.; Grünblatt, E.; Maor, G.; Youdim, M.B.H. Early and Late Gene Changes in MPTP Mice Model of Parkinson’s Disease Employing cDNA Microarray. *Neurochem. Res.* **2002**, *27*, 1231–1243. [[CrossRef](#)]
120. Lin, Q.-S.; Chen, P.; Wang, W.-X.; Lin, C.-C.; Zhou, Y.; Yu, L.-H.; Lin, Y.-X.; Xu, Y.-F.; Kang, D.-Z. RIP1/RIP3/MLKL Mediates Dopaminergic Neuron Necroptosis in a Mouse Model of Parkinson Disease. *Lab. Investig.* **2020**, *100*, 503–511. [[CrossRef](#)]
121. Oliveira, S.R.; Dionísio, P.A.; Gaspar, M.M.; Ferreira, M.B.T.; Rodrigues, C.A.B.; Pereira, R.G.; Estevão, M.S.; Perry, M.J.; Moreira, R.; Afonso, C.A.M.; et al. Discovery of a Necroptosis Inhibitor Improving Dopaminergic Neuronal Loss after MPTP Exposure in Mice. *Int. J. Mol. Sci.* **2021**, *22*, 5289. [[CrossRef](#)]
122. Meredith, G.E.; Totterdell, S.; Beales, M.; Meshul, C.K. Impaired Glutamate Homeostasis and Programmed Cell Death in a Chronic MPTP Mouse Model of Parkinson’s Disease. *Exp. Neurol.* **2009**, *219*, 334–340. [[CrossRef](#)]
123. Jackson-Lewis, V.; Jakowec, M.; Burke, R.E.; Przedborski, S. Time Course and Morphology of Dopaminergic Neuronal Death Caused by the Neurotoxin 1-Methyl-4-Phenyl-1,2,3,6-Tetrahydropyridine. *Neurodegeneration* **1995**, *4*, 257–269. [[CrossRef](#)] [[PubMed](#)]
124. Kolacheva, A.A.; Kozina, E.A.; Volina, E.V.; Ugryumov, M.V. Time Course of Degeneration of Dopaminergic Neurons and Respective Compensatory Processes in the Nigrostriatal System in Mice. *Dokl. Biol. Sci.* **2014**, *456*, 160–164. [[CrossRef](#)] [[PubMed](#)]

Disclaimer/Publisher’s Note: The statements, opinions and data contained in all publications are solely those of the individual author(s) and contributor(s) and not of MDPI and/or the editor(s). MDPI and/or the editor(s) disclaim responsibility for any injury to people or property resulting from any ideas, methods, instructions or products referred to in the content.